10-1992

# Interaction of Profiled Light with Contrapropagating Acoustic Waves: Fourier Transform Approach

Partha P. Banerjee
*University of Dayton*, pbanerjee1@udayton.edu

Chen-Wen Tarn
*National Taiwan University of Science and Technology*

Jaw-Jueh Liu
*University of Alabama, Huntsville*

### eCommons Citation

Banerjee, Partha P.; Tarn, Chen-Wen; and Liu, Jaw-Jueh, "Interaction of Profiled Light with Contrapropagating Acoustic Waves: Fourier Transform Approach" (1992). *Electrical and Computer Engineering Faculty Publications*. 188.
https://ecommons.udayton.edu/ece_fac_pub/188

# Interaction of profiled light with contrapropagating acoustic waves: a Fourier transform approach

**Partha P. Banerjee**
**Chen-Wen Tarn**
**Jaw-Jueh Liu**
University of Alabama in Huntsville
Department of Electrical and Computer
  Engineering
Optical Information Processing Laboratory
Optics Building
Huntsville, Alabama 35899

**Abstract.** A straightforward Fourier-transform approach is employed to investigate acousto-optic interaction between an input optical beam with arbitrary profile and contrapropagating cw sound in the Bragg regime. The process can be analyzed in terms of the simultaneous scattering of light by the two sound waves in the interaction region. Analytic expressions for the equivalent transfer functions are obtained and the scattered light profiles are plotted.

## 1 Introduction

In previous publications[1,2] we have used a Fourier-transform technique in conjunction with multiple plane wave scattering theory[3,4] to describe the acousto-optic (AO) interaction of light beams having arbitrary amplitude and phase profiles with cw and pulsed ultrasound, in terms of transfer functions relating the spatio-temporal spectra of the scattered light to the spatial spectrum of the input light profile. The Fourier-transform technique we have used is similar to the method employed for solving the paraxial wave equation.[5] The transfer functions derived clearly bring out the effects of AO interaction and propagational diffraction, and show how the interaction coefficients may be modified because of the latter effect. Our results for the interaction between profiled light and cw sound compare favorably with the analysis of Chatterjee et al.[6] (which does not take propagational diffraction into account) and can be readily derived from Korpel's analysis,[7] which employs the concept of the so-called virtual angular plane wave spectrum. The concept of the transfer function has also been used in connection with the analysis of apodized AO Bragg cells.[8] The rigorous comparison between different analytic methods used by various groups of researchers in the area, and details of the derivation of our analytical approach (as in Refs. 1 and 2), and that of Korpel[7] will be presented elsewhere.[9] The transfer function approach has also been successfully used to assess the effect of various sources of noise in AO devices and, on a related note, in the performance of photorefractive volume holograms.[10]

In this paper, we use the same Fourier transform technique to analyze the problem of an incident light beam undergoing Bragg scattering by contrapropagating acoustic waves in an AO medium. A special case of this is a standing wave AO modulator, which is used quite often in the active mode-locking of lasers, and in intensity modulation of laser

beams.[11,12] The standing wave can be considered to be a superposition of equal amplitude acoustic waves propagating in opposite directions. To give readers some physical insight into the problem, the heuristic photon-photon collision model of AO interaction leading to conservation laws of momentum and energy is first presented in Sec. 2. We consider the so-called multiple scattering model and show how even in the case of Bragg diffraction, one can get different up- or down-shifted frequencies of light in the same scattered direction. Subsequently, for a more precise formulation, a set of coupled differential equations are derived from the wave equation to describe the corresponding interaction between the scattered orders at different frequencies.

In Sec. 3, we use the Fourier-transform technique to express the coupled equations in the spatial frequency domain. Two different sets of analytic solutions are then presented in terms of transfer functions which relate the output spectra of the scattered orders to the input light spectrum. The first set corresponds to the case where the amplitudes of the contrapropagating sound waves in the AO interaction region are equal and give rise to a standing acoustic wave pattern. Our results, which compare favorably with those in Haus,[11] are expressible in terms of Bessel functions of different orders. The order of the Bessel function is commensurate with the amount of frequency shift of the output scattered light. This approach takes into account the multiple scattering of the different frequency components, and essentially serves as a check of our formulation of the problem. In the second case, we restrict ourselves to two scatterings only, realizing that the contributions from higher order scattering may be neglected under appropriate assumptions for the sound field amplitudes. In this case, we use the derived transfer functions to compute the output profiles of the light emanating in different directions. The composite profiles depend not only on the amplitudes of the contradirected sound, but are also functions of time. These results are shown in Sec. 4. Our conclusions are presented in Sec. 5.
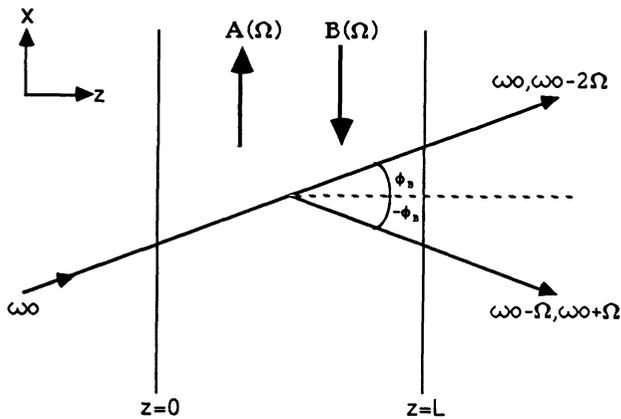
Fig. 1 Interaction between light and contradirected sound in the Bragg regime.

## 2 Heuristic Bragg Regime Analysis and General Formalism

As a heuristic background, we first use the momentum and energy conservation laws[7] to determine the direction and frequency of each component of the scattered light interacting with the contradirected sound in the Bragg regime. The overall acoustic signal responsible for the scattering can be considered in general as a superposition of two acoustic waves with same frequency but different amplitudes propagating in opposite directions, as shown in Fig. 1. The acoustic wave $A$ propagating along the $+x$ direction diffracts the light, nominally incident at the Bragg angle $+\phi_B$, and at frequency $\omega_0$, into the $-1$ order, which has a frequency $\omega_0 - \Omega$ and travels at an angle $-\phi_B$, where $\Omega$ is the sound frequency. All angles mentioned in this paper are with respect to the $z$ axis. Similarly, the sound wave $B$, propagating along $-x$, generates the $+1$-order light, which has a frequency $\omega_0 + \Omega$ and propagates along the same direction as the $-1$ order. Furthermore, in the case of strong interaction, the acoustic wave $B$ rescatters the diffracted light $(\omega_0 - \Omega)$ into the $-2$ order, which has a frequency $\omega_0 - 2\Omega$ and propagates along the same direction as the incident, or 0-order light.

Note that subsequent multiple scatterings will generate two groups of scattered light. The first group comprises the frequencies $\omega_0 - 2n\Omega$, where $n$ is an integer, and propagates at an angle $+\phi_B$. The second group comprises light at frequencies $\omega_0 - (2n+1)\Omega$, and propagates at an angle $-\phi_B$. Thus, every direction, $\pm\phi_B$, has different frequency components of the scattered light field, leading to intensity modulation of the light in time, which can be observed at all distances to the right of the AO cell that are smaller than the coherence length of the output light, typically of the order of $c\Omega \approx 10$ m.

To quantitatively predict the spatial profile of the intensity modulated light, we start from the wave equation for a TE optical field in a medium with constant permeability $\mu_0$ and whose permittivity $\varepsilon(x, z, t) = \varepsilon_0 + \varepsilon'(x, z, t)$ is a slowly varying function of $x$, and $z$, and $t$:

$$\nabla^2 E(x, z, t) - \mu_0 \varepsilon_0 \frac{\partial^2 E(x, z, t)}{\partial t^2} \cong \mu_0 \varepsilon'(x, z, t) \frac{\partial^2 E(x, z, t)}{\partial t^2} \ .$$

$$(1)$$

We now write

$$\varepsilon'(x, z, t) = \tfrac{1}{2}\varepsilon_0 C[A \exp(-jKx) + B \exp(jKx)]$$
$$\times \exp(j\Omega t) + \text{c.c.} \ , \qquad (2)$$

where c.c. denotes the complex conjugate. $A$ and $B$ denote the amplitudes of the contrapropagating components of the sound in the AO interaction region. $C$ is an interaction constant and $K$ is the propagation constant for the sound. Also, following our heuristic development, we write

$$E_{\text{inc}}(x, z, t) = \tfrac{1}{2}\psi_{\text{inc}}(x, z) \exp(j\omega_0 t)$$
$$\times \exp(-jk_0 z \cos\phi_B) + \text{c.c.} \ , \qquad (3)$$

$$E(x, z, t) = \tfrac{1}{2} \sum_{n=-\infty}^{\infty} [\psi_{2n}(x, z) \exp(j(\omega_0 + 2n\Omega)t)$$
$$\times \exp(-jk_0 z \cos\phi_0 - jk_0 x \sin\phi_0)$$
$$+ \psi_{2n+1}(x, z) \exp[j(\omega_0 + (2n+1)\Omega)t]$$
$$\times \exp(-jk_0 z \cos\phi_{-1} - jk_0 x \sin\phi_{-1}) + \text{c.c.} \ , \qquad (4)$$

where $E_{\text{inc}}$ is the optical field incident on the sound column. Furthermore, from our previous discussion, it is clear that $\phi_0 = \phi_B$, $\phi_{-1} = -\phi_B$, where $\sin\phi_B = K/2k_0$ and $k_0$ is the propagation constant for the light.

Substituting (2) and (4) into (1), assuming $\Omega \ll \omega_0$, and collecting terms with same carrier frequency, we have, after considerable algebra,

$$\frac{\partial^2 \psi_{2n}}{\partial x^2} + \frac{\partial^2 \psi_{2n}}{\partial z^2} - 2jk_0 \sin\phi_B \frac{\partial \psi_{2n}}{\partial x} - 2jk_0 \cos\phi_B \frac{\partial \psi_{2n}}{\partial z}$$
$$+ \tfrac{1}{2}k_0^2 CA\psi_{2n-1} + \tfrac{1}{2}k_0^2 CB^*\psi_{2n-1} = 0 \qquad (5)$$

and

$$\frac{\partial^2 \psi_{2n+1}}{\partial x^2} + \frac{\partial^2 \psi_{2n+1}}{\partial z^2} + 2jk_0 \sin\phi_B \frac{\partial \psi_{2n+1}}{\partial x}$$
$$- 2jk_0 \cos\phi_B \frac{\partial \psi_{2n+1}}{\partial z}$$
$$+ \tfrac{1}{2}k_0^2 CB\psi_{2n} + \tfrac{1}{2}k_0^2 CA^*\psi_{2n+2} = 0 \ . \qquad (6)$$

Using these coupled equations, we can describe the interaction of a light profile with contrapropagating sound more precisely. Equation (5) describes the evolution of all components of scattered light traveling nominally at $+\phi_B$ for an input profile nominally incident at $+\phi_B$. Similarly, Eq. (6) describes all components traveling nominally at $-\phi_B$. The physical interpretation is as follows: The evolution of, say, the 0-order light in $z$ depends on (1) the interaction between $-1$ order with the acoustic wave $A$ (the fifth term on the LHS of Eq. (5)), (2) the interaction between the $+1$ order with the acoustic wave $B^*$ (the sixth term on the LHS), (3) the effect of propagational diffraction (the first term on the LHS). The third term on the LHS of Eq. (5) is merely the effect of the 0-order light traveling in a direction slightly different from its nominal direction $+\phi_B$. Reasons for this departure from the heuristic model may be found in Refs.

1 and 6. A similar physical interpretation can be advanced for all other frequency components that nominally travel at $+\phi_B$, as well as for those components that nominally travel at $-\phi_B$, using Eq. (6). Note that by setting $B=0$ or $A=0$, we can reduce Eqs. (5) and (6) to forms that are identical to those found in Ref. 1. In this case, however, the light exiting at $\pm \phi_B$ contains only one frequency.

## 3 The Fourier Transform Approach and the Spatial Transfer Function

We now employ a Fourier transform technique to express the interaction described by Eqs. (5) and (6) in the spatial frequency domain. To this end, we define the Fourier transform pair:

$$\Psi_n(k_x, z) = F[\psi_n(x, z)] = \int_{-\infty}^{\infty} \psi_n(x, z) \exp(jk_x x) \, dx \ , \tag{7}$$

$$\psi_n(x, z) = F^{-1}[\Psi_n(k_x, z)] = \frac{1}{2\pi} \int_{-\infty}^{\infty} \Psi_n(k_x, z)$$
$$\times \exp(-jk_x x) \, dk_x \ , \tag{8}$$

where $k_x$ is the spatial frequency variable corresponding to $x$. The method used is identical to the technique for solving the paraxial wave equation to derive the transfer function of propagation and, hence, the Fresnel diffraction formula during free-space propagation of a light beam in the presence of diffraction.[5]

The coupled differential equations in the spatial frequency domain are

$$\frac{d\Psi_{2n}(k_x, z)}{dz} = j \frac{k_x^2 + 2k_0 k_x \sin\phi_B}{2k_0 \cos\phi_B} \Psi_{2n}(k_x, z)$$

$$-j \frac{k_0 CA}{4 \cos\phi_B} \Psi_{2n-1}(k_x, z)$$

$$-j \frac{k_0 CB^*}{4 \cos\phi_B} \Psi_{2n+1}(k_x, z) \ , \tag{9}$$

and

$$\frac{d\Psi_{2n+1}(k_x, z)}{dz} = j \frac{k_x^2 - 2k_0 k_x \sin\phi_B}{2k_0 \cos\phi_B} \Psi_{2n+1}(k_x, z)$$

$$-j \frac{k_0 CB}{4 \cos\phi_B} \Psi_{2n}(k_x, z)$$

$$-j \frac{k_0 CA^*}{4 \cos\phi_B} \Psi_{2n+2}(k_x, z) \ , \tag{10}$$

where we have assumed "slow" variation of $\psi_n$ (and hence $\Psi_n$) with respect to $z$, enabling us to neglect second derivatives with respect to $z$.

There is no analytic solution for these coupled equations, unless some assumptions are made. In this paper, we solve (9) and (10) for two illustrative cases, mentioned below. For each case, we can derive the spatial transfer functions

that relate the output spectra of the scattered orders to the input spectrum of arbitrary beam profile. It is convenient to track these relationships along $z'$ and $z''$, which are the nominal directions of propagation, at angles $\pm \phi_B$, with respect to $z$. The directions orthogonal to $z'$ and $z''$ are $x'$ and $x''$, respectively, and $k_{x'}$ and $k_{x''}$ denote the corresponding spatial frequencies. Details of the coordinate transformation and its effect on the derivation of the transfer functions may be excavated from Ref. 1. This helps us derive the interaction transfer functions $H_{2n}(k_{x'}; z''/L)$ and $H_{2n+1}(k_{x''}; z''/L)$ in the presence of propagational diffraction and, hence, the scattered light profiles at different frequencies using the relations

$$\psi_{2n}(x', z'/L) = \frac{1}{2\pi} \int_{-\infty}^{\infty} \Psi_{inc}(k_{x'}; z'/L) H_{2n}(K_{x'}; z'/L)$$
$$\times \exp(-jk_{x'}x') \, dk_{x'} \ , \tag{11}$$

$$\psi_{2n+1}(x'', z''/L) = \frac{1}{2\pi} \int_{-\infty}^{\infty} \Psi_{inc}(k_{x''}; z''/L) H_{2n+1}$$
$$\times (k_{x''}; z''/L) \exp(-jk_{x''}x'') \, dk_{x''} \ , \tag{12}$$

where

$$x' = x \cos\phi_B - z \sin\phi_B, \quad z' = x \sin\phi_B + z \cos\phi_B \ , \tag{13}$$

$$x'' = x \cos\phi_B + z \sin\phi_B \ , \quad z'' = -x \sin\phi_B + z \cos\phi_B \ . \tag{14}$$

Note that in Eqs. (11) and (12), the integrands without the exponential terms are respectively equal to $\Psi_{2n}(k_{x'}; z'/L)$ and $\Psi_{2n+1}(k_{x''}; z''/L)$, which are the Fourier transforms of the scattered light profiles $\psi_{2n}$ and $\psi_{2n+1}$.

### Case 1: A = B

By assuming $A = B =$ a real constant, we can solve (9) and (10) to express $\Psi_{2n}$, $\Psi_{2n+1}$ in terms of $\Psi_{inc}$, and hence derive the transfer functions $H_{2n}(k_{x'}; z')$ and $H_{2n+1}(k_{x''}; z'')$, after straightforward but tedious algebra, as

$$H_{2n}(k_{x'}; z') = (-j)^{2n} \exp[j(k_{x'}^2 z'/2K_0 - \phi_B k_{x'}z')]$$
$$\times J_{2n}\left\{ \frac{k_0 CAz'}{2 \cos\phi_B} \left[ \frac{\sin(\phi_B k_{x'}z')}{\phi_B k_{x'}z'} \right] \right\} \ , \tag{15}$$

$$H_{2n+1}(k_{x''}; z'') = (-j)^{2n+1} \exp[j(k_{x''}^2 z''/2K_0 + \phi_B k_{x''}z'')]$$
$$\times J_{2n+1}\left\{ \frac{k_0 CAz''}{2 \cos\phi_B} \left[ \frac{\sin(\phi_B k_{x''}z'')}{\phi_B k_{x''}z''} \right] \right\} \ . \tag{16}$$

The calculations involved in the derivation of the transfer functions are somewhat similar to those encountered in the derivation of the transfer function for the case of light scattering in the Raman-Nath regime for unidirectional propagating sound, as shown in Ref. 13. The first part of each exponential in (15) and (16) represents the effects of prop-

agational diffraction, with the second part denoting a small spatial shift in the far field, similar to earlier observations in Refs. 1 and 6. The transfer functions have been expressed with $z'$ and $z''$ as parameters, instead of $z'/L$ and $z''/L$ to enable easier comparison with Haus.[11] For plane wave incidence (for the light), $\psi_{\text{inc}} = 1$, implying $\Psi_{\text{inc}} = \delta(k_x)$, and $\psi_{2n}$ and $\psi_{2n+1}$ become $(-j)^{2n}J_{2n}(k_0CAz'/2 \cos\phi_B)$ and $(-j)^{2n+1}J_{2n+1}(k_0CAz''/2 \cos\phi_B)$, in agreement with the results in Ref. 11. The above example thus serves as a check of our mathematical formulation thus far.

## Case 2: $\mathbf{A} \neq \mathbf{B}$

In case 1, note that at the exit of the sound cell ($z' \approx z'' \approx L$), the argument of the Bessel functions is equal to the peak phase delay $\alpha = k_0CAL/2$ ($\phi_B$ small) encountered by the light during its passage through the sound cell. Accordingly, for reasonably small $\alpha(\leq \pi/2)$, the contributions from scattered light for $|n| \geq 3$ are negligibly small when compared to that resulting from lower values of $|n|$. Thus, in this case, we restrict ourselves to the scattered orders $\psi_0$, $\psi_1$, $\psi_{-1}$, and $\psi_{-2}$. We remind readers that $\psi_0$ and $\psi_{-2}$ propagate at an angle $+\phi_B$ for light incident at the same angle, while $\psi_1$ and $\psi_{-1}$ propagate nominally at $-\phi_B$. We can now write the evolution equations for these components in the spatial frequency domain using (9) and (10). Note that, for instance, the evolution of the 0 order depends on the $\pm 1$ orders, while that for $-2$ and $+1$ depends on the $-1$ and 0 orders, respectively. The contributions to the $-1$ order come from the 0 and $-2$ orders. However, realizing that the $-2$ order should be much smaller than any of the other orders, we may neglect the contribution from the $-2$ order toward the evolution of the $-1$ order. This assumption turns out to be a valid one, as is realized from examining the derived transfer function $H_{-2}$. Furthermore, the assumption helps us write the interaction transfer functions elegantly in closed form and in a manner reminiscent of the transfer functions derived in Ref. [1] for Bragg scattering of light by unidirectional cw sound. After straightforward but lengthy algebra, these transfer functions may be written as

$$H_0(k_{x'}, z'/L) = \exp[j(k_{x'}^2L/2k_0 - k_{x'}Q\Lambda/4\pi)z'/L]$$

$$\times \{\cos[(k_{x'}Q\Lambda/4\pi)^2 + (\alpha_1/2)^2 + (\alpha_2/2)^2]^{1/2}z'/L$$

$$+ j\frac{k_{x'}Q\Lambda/4\pi}{[(k_{x'}Q\Lambda/4\pi)^2 + (\alpha_1/2)^2 + (\alpha_2/2)^2]^{1/2}}$$

$$\times \sin[(k_{x'}Q\Lambda/4\pi)^2 + (\alpha_1/2)^2 + (\alpha_2/2)^2]^{1/2}z'/L\} , \quad (17)$$

$$H_{-1}(k_{x''}, z''/L) = -j \exp[j(k_{x''}^2L/2k_0 + k_{x''}Q\Lambda/4\pi)z''/L]$$

$$\times \left\{ \frac{(\alpha_1/2)\exp-j(\arg A)}{[(k_{x''}Q\Lambda/4\pi)^2 + (\alpha_1/2)^2 + (\alpha_2/2)^2]^{1/2}} \right.$$

$$\times \sin[(k_{x''}Q\Lambda/4\pi)^2 + (\alpha_1/2)^2 + (\alpha_2/2)^2]^{1/2}z''/L \bigg\} , \quad (18)$$

$$H_{+1}(k_{x''}, z''/L) = -j \exp[j(k_{x''}^2L/2k_0 + k_{x''}Q\Lambda/4\pi)z''/L]$$

$$\times \left\{ \frac{(\alpha_2/2)\exp j(\arg B)}{[(k_{x''}Q\Lambda/4\pi)^2 + (\alpha_1/2)^2 + (\alpha_2/2)^2]^{1/2}} \right.$$

$$\times \sin[(k_{x''}Q\Lambda/4\pi)^2 + (\alpha_1/2)^2 + (\alpha_2/2)^2]^{1/2}z''/L \bigg\} , \quad (19)$$

$$H_{-2}(k_{x'}, z'/L) = \exp[j(k_{x'}^2L/2k_0 - k_{x'}Q\Lambda/4\pi)z'/L$$

$$- j(\arg A + \arg B)]$$

$$\times \frac{\alpha_1\alpha_2}{\alpha_1^2 + \alpha_2^2} \left\{ \cos[(k_{x'}Q\Lambda/2\pi)^2 + (\alpha_1/2)^2 + (\alpha_2/2)^2]^{1/2}z'/L \right.$$

$$+ j\frac{k_{x'}Q\Lambda/4\pi}{[(k_{x'}Q\Lambda/4\pi)^2 + (\alpha_1/2)^2 + (\alpha_2/2)^2]^{1/2}}$$

$$\times \sin[(k_{x'}Q\Lambda/4\pi)^2 + (\alpha_1/2)^2 + (\alpha_2/2)^2]^{1/2}z'/L - 1\bigg\} , \quad (20)$$

where $x'$, $z'$ and $x''$, $z''$ are defined in (13) and (14).

The quantities $\alpha_1(= k_0C|A|L/2)$ and $\alpha_2(= k_0C|B|L/2)$ denote the peak phase delays encountered by the light during its passage through the sound waves $A$ and $B$, respectively, and $\arg A$, $\arg B$ denote the phases of $A$ and $B$, respectively. Also, $\Lambda$ is the wavelength of sound in the interaction region and $Q = K^2L/k$ is the Klein-Cook parameter. This time we express the transfer functions in terms of $z'/L$ and $z''/L$ for purposes of comparison with Ref. 1.

From the transfer functions (15) derived from the Fourier-transform technique as above, we find out that the output profile of each scattered light beam depends not only on the forward-traveling sound wave $A(\alpha_1)$, but also the backward-traveling wave $B(\alpha_2)$. It can be readily seen that $|H_{-2}| < < |H_0|$ if $\alpha_2 < \alpha_1$. We also can observe the effects of propagational diffraction and spatial shifting as seen in the case of unidirectional cw sound. Also, by letting $\alpha_2 = 0$ (cw unidirectional sound), the transfer functions $H_0$ and $H_{-1}$ become identical to the ones derived in Ref. 1, while $H_{+1}$ and $H_{-2}$ become equal to zero, as expected.

## 4 Calculation Results and Discussion

We have computed the composite amplitude profiles $|\psi_0 + \psi_{-2} \exp(-j2\Omega t)|$ and $|\psi_1 \exp(j\Omega t) + \psi_{-1} \exp(-j\Omega t)|$ in the $+\phi_B$ and $-\phi_B$ directions, respectively, at the exit of the AO interaction region ($z = L$) for various values of $\alpha_1$ and $\alpha_2$, as well as for various values of the phase difference $\Delta\theta$ between the forward- and backward-traveling sound waves $A$ and $B$, respectively, and as functions of time. We remark, in passing, that the "far-field" profiles can also be readily calculated by deleting the integrations in (11) and (12) and by replacing $k_{x'}$ by $k_0x'/z'$ and $k_{x''}$ by $k_0x''/z''$. Figures 2(a) and (b) show three-dimensional plots of the composite profiles along $+\phi_B$ and $-\phi_B$, respectively, for $Q = 8$, $\alpha_1 = 0.4\pi$, $\Delta\theta = 0$, and at $t = 0$, as $\alpha_2$ varies from 0 to $0.2\pi$. In this
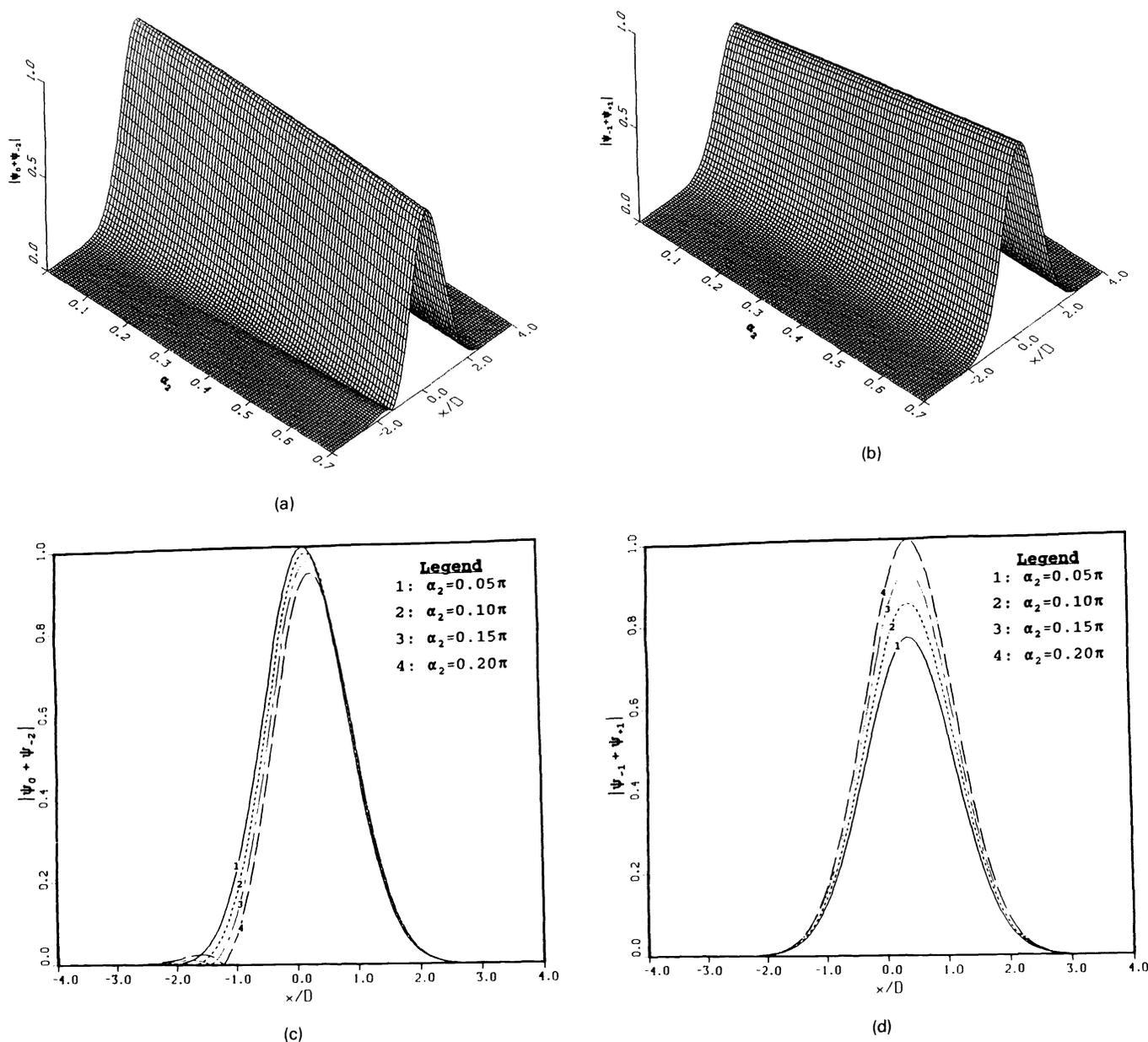
(a)



(b)



(c)



(d)

**Fig. 2** (a) Three-dimensional plot showing variation of composite profile in the $+\phi_B$ direction as functions of $\alpha_2$ and $x/D$ for $Q=8$, $\alpha_1=0.4\pi$, $\Delta\theta=0$, and at $t=0$. (b) Three-dimensional plot showing variation of composite profile in the $-\phi_B$ direction as functions of $\alpha_2$ and $x/D$ for $Q=8$, $\alpha_1=0.4\pi$, $\Delta\theta=0$, and at $t=0$. (c) Cross-sectional plots of (a) for $\alpha_2=0.05\pi$, $0.1\pi$, $0.15\pi$, and $0.2\pi$. (d) Cross-sectional plots of (b) for $\alpha_2=0.05\pi$, $0.1\pi$, $0.15\pi$, and $0.2\pi$.

figure and in all subsequent plots, we assume an incident Gaussian beam of waist size $D=2\Lambda$, where $\Lambda$, the wavelength of sound, is $0.128\times10^{-3}$m; $\lambda_0$ = wavelength of light $=0.632\times10^{-6}$m, and $L=5$ cm. We assume, for simplicity, that the refractive index of the AO cell is equal to 1. Figures 2(c) and (d) are representative cross sections from Figs. 2(a) and (b), respectively, and show that the composite amplitude peak along $-\phi_B$ increases as $\alpha_2$ increases. Note the small distortion in the composite profile along $+\phi_B$ as $\alpha_2$ is increased. This may also be interpreted as a gradual narrowing of the profile with increase in $\alpha_2$, as may be verified by measuring the width (distance between the $1/e$ points) of each of the curves.

A representative set of plots showing the dependence of the profiles on the phase difference $\Delta\theta$ and at $t=0$ is shown in Figs. 3(a) through 3(d) for $\alpha_1=0.4\pi$ and $\alpha_2=0.2\pi$. The sequence of figures is maintained the same as in the set of plots in Figs. 2(a) through 2(d). Note the decrease in the composite peak along $-\phi_B$ when $\Delta\theta=\pi$. The reason for this is clear if one reexamines the derived transfer functions (18) and (19) in this case. It is clearly seen that $H_1$ is now proportional to $H_{-1}$ but opposite in sign, so that at $t=0$, the output profile, which is proportional to $|F^{-1}[(H_{-1}+H_1)\Psi_{inc}]|$, is a minimum. The distortion in the composite profile along $+\phi_B$ for $\Delta\theta=2\pi$ (or 0) is also visible.

(a)


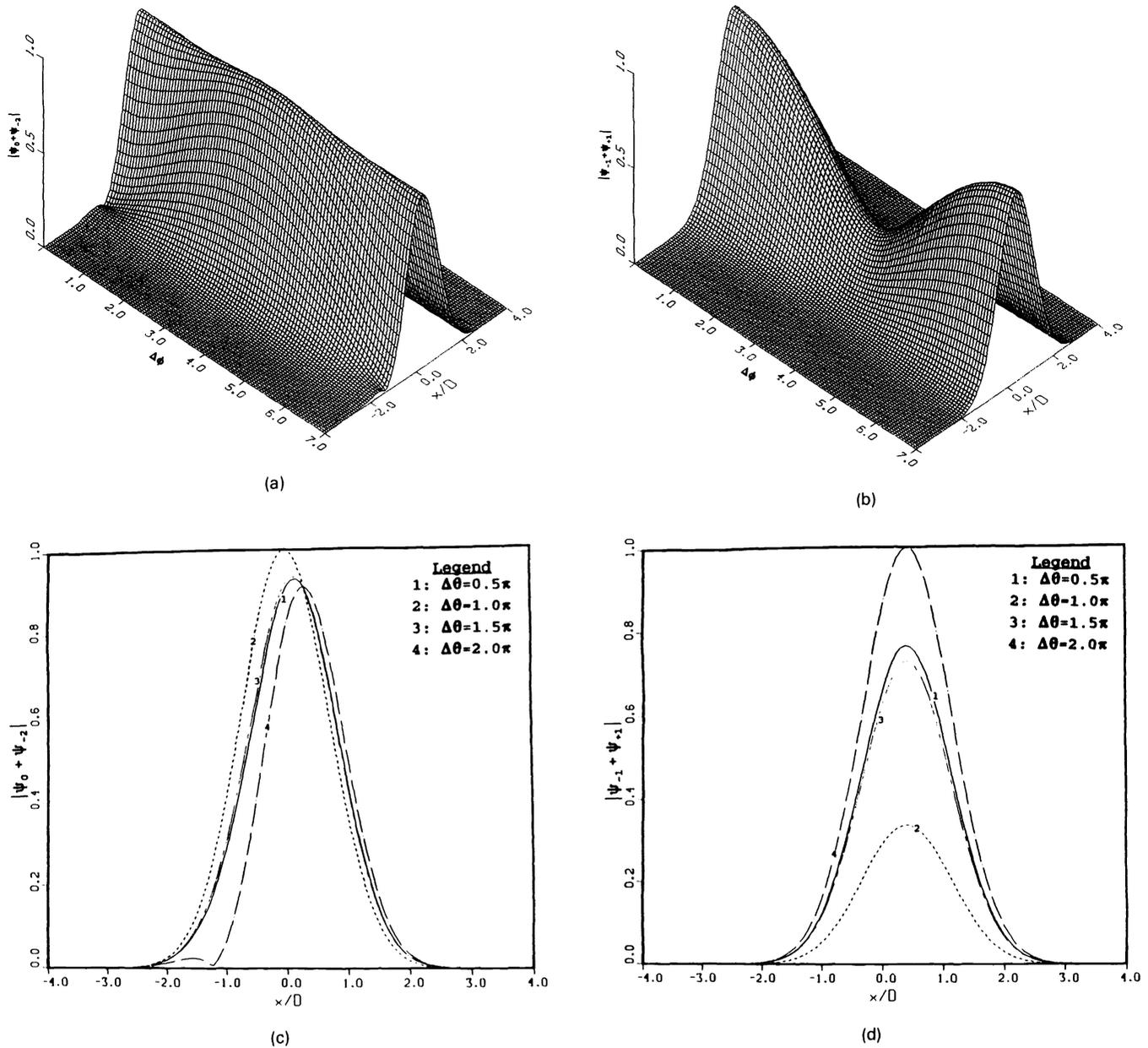
(b)



(c)



(d)

**Fig. 3** (a) Three-dimensional plot showing variation of composite profile in the $+\phi_B$ direction as functions of $\Delta\theta$ and $x/D$ for $Q=8$, $\alpha_1=0.4\pi$, $\alpha_2=0.2\pi$, and at $t=0$. (b) Three-dimensional plot showing variation of composite profile in the $-\phi_B$ direction as functions of $\Delta\theta$ and $x/D$ for $Q=8$, $\alpha_1=0.4\pi$, $\alpha_2=0.2\pi$, and at $t=0$. (c) Cross-sectional plots of (a) for $\Delta\theta=0.5\pi$, $\pi$, $1.5\pi$, and $2\pi$. (d) Cross-sectional plots of (b) for $\Delta\theta=0.5\pi$, $\pi$, $1.5\pi$, and $2\pi$.

Finally, we show plots of the output profiles as a function of time for $\alpha_1=0.4\pi$ and $\alpha_2=0.2\pi$ in Figs. 4(a) through 4(d). It is important to note that the output profiles vary periodically as a function of time, and that the maximum intensity in the $-\phi_B$ direction occurs at $t=\pi/\Omega$ or 0. At this time, the profile along $+\phi_B$ also exhibits the maximum distortion and narrowing. The minimum intensity along $-\phi_B$ occurs at $t=\pi/2\Omega$. The intensities are, therefore, time modulated with a modulation frequency $2\Omega$. Thus, a good quality, constant width, time-modulated intensity profile can be obtained in the $-\phi_B$ direction using contradirected sound fields by making $\alpha_2$ as large as possible and by ensuring

$\Delta\theta=0$. The depth of modulation (or modulation index) for this intensity profile is roughly proportional to the ratio $\alpha_2/\alpha_1 = |B|/|A|$.

## 5 Conclusion

A straightforward Fourier-transform approach has been developed to solve the light–sound interaction problem between an input optical beam with arbitrary initial profile and contrapropagating sound waves in the Bragg regime. Analytic expressions for the interaction transfer function of each scattered order light is presented, and the nature of the
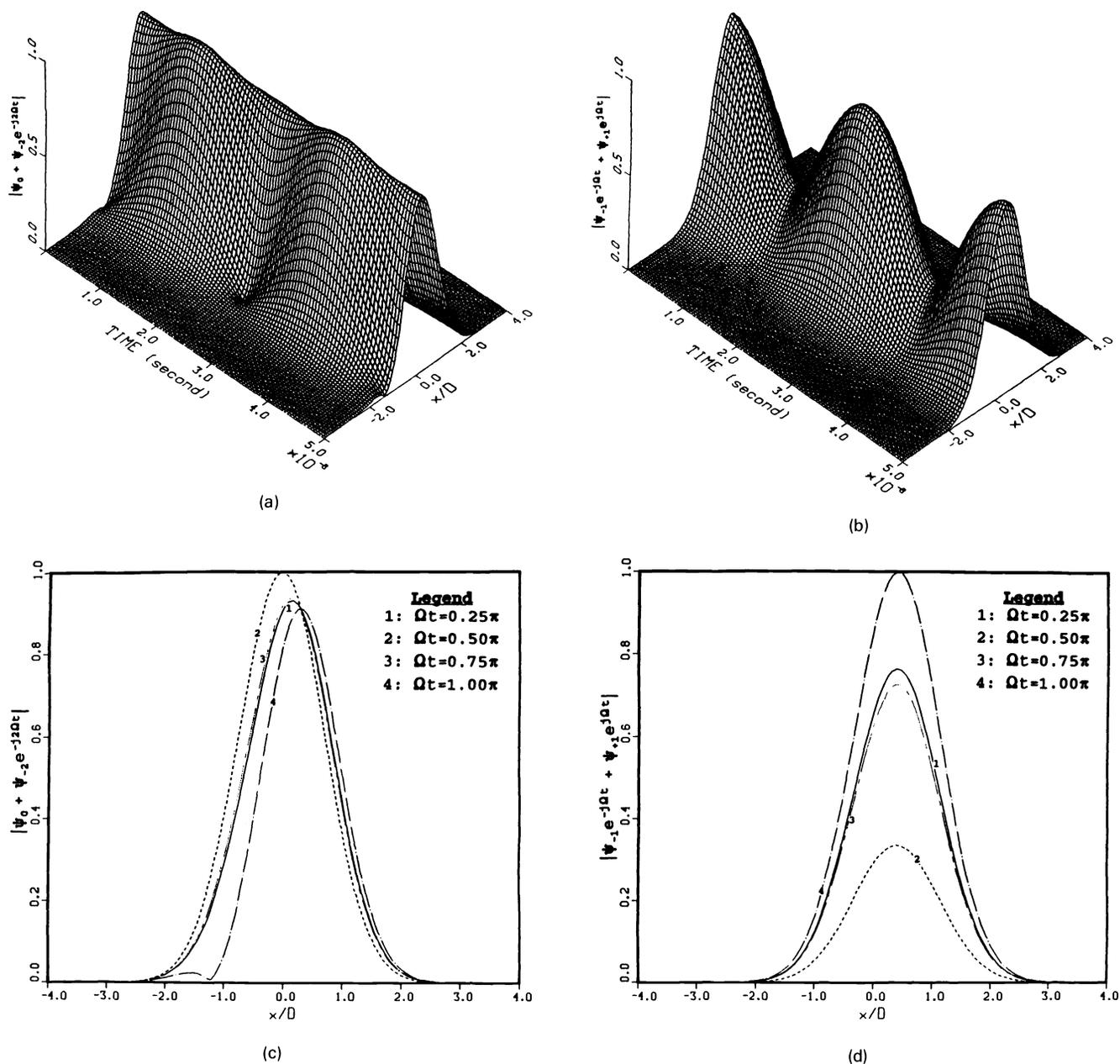
(a)



(b)



(c)



(d)

**Fig. 4** (a) Three-dimensional plot showing variation of composite profile in the $+\phi_B$ direction as functions of time and $x/D$ for $Q = 8$, $\alpha_1 = 0.4\pi$, and $\alpha_2 = 0.2\pi$. (b) Three-dimensional plot showing variation of composite profile in the $-\phi_B$ direction as functions of time and $x/D$ for $Q = 8$, $\alpha_1 = 0.4\pi$, and $\alpha_2 = 0.2\pi$. (c) Cross-sectional plots of (a) for $\Omega t = 0.25\pi$, $0.5\pi$, $0.75\pi$, and $\pi$. (d) Cross-sectional plots of (b) for $\Omega t = 0.25\pi$, $0.5\pi$, $0.75\pi$, and $\pi$.

output intensity modulated beam is studied. Criteria for obtaining a good quality, time-modulated intensity profile are presented. The transfer functions derived will be used to assess the performance of AO devices in the presence of noise where we can include the effect(s) of any possible backscatter of the propagating sound in a commonly used AO cell. Work on this is currently in progress.
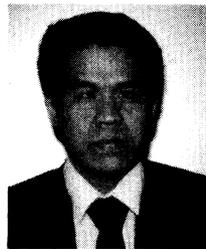
## Acknowledgment

## References

1. P. P. Banerjee and C. W. Tarn, "A Fourier transform approach to acousto-optic interactions in the presence of propagational diffraction," *Acustica* **74**, 181–191 (1991).
2. C. W. Tarn and P. P. Banerjee, "A spatio-temporal Fourier-transform to acousto-optic interaction of light beams with cw and pulsed ultrasonic waves," *Opt. Commun.* **85**, 481–490 (1991).
3. A. Korpel, "Two-dimensional plane wave theory of strong acousto-optic interaction in isotropic media," *J. Opt. Soc. Am.* **69**, 678–683 (1979).
4. A. Korpel and T.-C. Poon, "Explicit formalism for acousto-optic multiple plane-wave scattering," *J. Opt. Soc. Am.* **70**, 817–820 (1980).
5. P. P. Banerjee and T.-C. Poon, *Principles of Applied Optics,* Irwin, Boston (1991).
6. M. R. Chatterjee, T.-C. Poon and D. N. Sitter, "Transfer function

formalism for strong acousto-optic Bragg diffraction of light beams with arbitrary profile," *Acustica* **71**, 81–89 (1990).

7. A. Korpel, *Acousto-Optics*, Dekker, New York (1988).
8. R. J. Pieper and T.-C. Poon, "System characterization of apodized acousto-optic Bragg cells," *J. Opt. Soc. Am. A* **7**, 1751–1758 (1990).
9. A. Korpel, P. P. Banerjee, and C. W. Tarn, "A unified treatment of special formalisms of light propagation and their application to acousto-optics," submitted to *Opt. Commun*.
10. A. K. Ghosh, P. P. Banerjee, J.-J. Liu, and Q. W. Song, "The effect of noise on photorefractive grating readout," *Proc. SPIE* 1622 (1992).
11. H. Haus, *Waves and Fields in Optoelectronics*, Prentice-Hall, Englewood Cliffs, NJ (1984).
12. A. K. Ghatak and K. Thyagarajan, *Optical Electronics*, Cambridge University Press, New York (1976).
13. C. W. Tarn, "A spatio-temporal Fourier-transform approach to acousto-optic interaction," Ph.D. Thesis, Syracuse University (1991).

**Chen-Wen Tarn** received a BS degree in electronic engineering from Tamkang University, Taiwan, in 1983 and a PhD in electrical engineering from Syracuse University in 1991. In 1991, he joined the Department of Electrical and Computer Engineering, University of Alabama, Huntsville, as a visiting assistant professor. His research interests are acousto-optics, volume holography, nonlinear optics, and optical signal processing.

**Partha P. Banerjee** is an associate professor of the Department of Electrical and Computer Engineering at the University of Alabama in Huntsville. Dr. Banerjee received his BTech degree at the Indian Institute of Technology and his MS and PhD degrees in electrical and computer engineering at the University of Iowa. He has published over 50 technical papers in a variety of areas, including nonlinear wave phenomena, nonlinear optics and acoustics, optical information processing, acousto-optics, optical computing, and electromagnetics. He has also given presentations on nonlinear optics and acousto-optics internationally. Dr. Banerjee consults for industry and teaches courses on optics for professionals. Dr. Banerjee is a recipient of an NSF Presidential Young Investigator award. He is a member of OSA and the Society of Industrial and Applied Mathematics and is a senior member of the Institute of Electrical and Electronics Engineers.

**Jaw-Jueh Liu** received a BS degree in communication engineering from Chiao-Tung University, Taiwan, in 1984 and an MS in electrical engineering from Syracuse University in 1990. He is now a research assistant in the Department of Electrical and Computer Engineering at the University of Alabama in Huntsville. His research interests are photorefractive materials, acousto-optics, and nonlinear optics.